Journal of Inorganic and General Chemistry
ZAAC
Zeitschrift für anorganische und allgemeine Chemie
www.zaac.wiley-vch.de
RESEARCH ARTICLE

DOI: 10.1002/zaac.202300168

Special Collection

Polycyclic aromatic hydrocarbon radical anions stabilized by a sodium diglyme cation complex

Natalie Eichstaedt,[a] Ingmar Pietsch,[a] Daniel Friedrich,*[a] and Josef Breu*[a]

Dedicated to Professor Michael Ruck on the occasion of his 60th birthday

Reduction of polycyclic aromatic hydrocarbons by sodium in the presence of the chelating ether diglyme in THF resulted in the formation of radical carbanion salts. The crystal structure of a Na(diglyme)$_2$pyrenide, a new member in this material class, was solved from single-crystal X-ray diffraction data. The green compound crystallizes in the monoclinic space group $P2_1/c$ with unit cell parameters of $a = 8.9908(4)$ Å, $b = 16.6367(8)$ Å, $c = 19.1723(7)$ Å, $\beta = 94.734(2)°$, $V = 2857.9(2)$ Å^3, and $Z = 4$ ($T = 20\,°C$).

Introduction

In recent years, the demand for energy storage systems for various technological applications has continuously increased worldwide.[1] Lithium-ion batteries are currently the most widely used energy source especially in mobile electronic devices and electric vehicles.[2] This high demand has led to a steep increase of the market price of lithium, an element with relatively limited availability. To mitigate these problems, efforts have been made to develop alternative metal-cation batteries.[3] The most promising alternative are sodium-ion batteries due to the chemical similarities between sodium and lithium, its high natural abundance, and thus affordable price.[4] Currently, sodium-ion battery technology is similar to lithium-ion batteries and various materials are being investigated as battery components.[5] Among the most promising anode materials for lithium-ion batteries is graphite due to its cheap production cost, high capacity and reliable cycle stability.[6] A major challenge of graphite as anode material for sodium-ion batteries is the low sodium uptake.[6c,7] One way to address this problem is to activate the intercalation of Na^+ into the graphene layers via co-intercalation with solvent molecules.[8] Reversible Na^+ intercalation into graphite has first been achieved by Jache and Adelhelm in 2014 using diethylene glycol dimethyl ether (diglyme) as electrolyte solvent.[9]

Glymes are oligoether with a repetition unit of CH_2–CH_2–O with terminating methoxy-groups. These oligoethers are capable of forming stable chelate complexes with a wide range of cations similar to crown ethers.[10] The number of the coordination sites is directly proportional to the length of the oligoether. For example, two diglyme (G2) molecules, $CH_3O(CH_2CH_2O)_2CH_3$, form a stable chelate complex with lithium[11] and sodium[11c,12] cations. Glyme complexes can also be used to stabilize otherwise highly unstable reactants such as carbanions of polycyclic aromatic hydrocarbons (PAHs), a molecule class containing more than one aromatic ring.[13] Such aromatic radical anions are used in macromolecular chemistry as initiators[14] or in organometallic chemistry as reducing agents.[15]

Due to the delocalized π-electron system, aromatic PAHs[16] are able to react with electron donors like alkali metals, forming aromatic radical anions,[17] first published by Berthelot,[18] documenting the reaction of potassium with different PAHs. As their redox potentials are only slightly lower than that of the graphite intercalation compound anion $[C_6]^-$ they moreover appear as good mimics for battery anodes.[19] Preparation and storage of these anions demand anhydrous and anaerobic conditions due to the kinetic instability of the radicals. Therefore, only few examples of alkali metal aromatic radical anion salts, e.g. K_2(naphthalene)$_2$(THF) and $[(K_2THF_3)$(anthracene)$_2]$ are isolated and characterized.[20] In these examples, the carbanions in the crystal structure are mostly stabilized by cation-solvent interactions. Using 18-crown-6 as complexing agents, Castillo *et al.*[21] managed to stabilize several radical anion salts with different alkali metal cations in solution. For the aforementioned glymes, carbanions such as napthalenide, antracenide and perlyenide could be stabilized in the solid state.[12]

In analogy to the established synthesis route via alkali metal reduction in THF, as published by Eichstaedt *et al.*,[22] we

[a] N. Eichstaedt, I. Pietsch, Dr. D. Friedrich, Prof. Dr. J. Breu
Faculty of Biology, Chemistry & Earth Sciences
Chair of Inorganic Colloids for Electrochemical Energy storage
Bavarian Battery Center
University of Bayreuth
95440 Bayreuth, Germany
E-mail: daniel.friedrich@uni-bayreuth.de
josef.breu@uni-bayreuth.de

Supporting information for this article is available on the WWW under https://doi.org/10.1002/zaac.202300168

This article is part of a Special Collection dedicated to Professor Michael Ruck on the occasion of his 60th birthday. Please see our homepage for more articles in the collection.

synthesized microcrystalline samples of the previously reported compounds, Na(G2)naphthalenide and Na(G2)anthracenide, as well as a new member, Na(G2)$_2$pyrenide, the first salt with Na-stabilized pyrenide with discrete anion/cation pairs, structurally characterized in the solid-state. In literature, crystal structure data of pyrenide anions is only available for 1D infinite sodium structures and a lithium compound with mixed pyrenide anions and pyrene.[23] In all these structures, however, the alkali metal is directly coordinating to the pyrenide anions.[24] We successfully grew single crystals of this new compound from saturated solutions and solved the crystal structure using single-crystal X-ray diffraction techniques. Complementary experiments using X-ray powder diffraction, analysis via titration, atomic absorption spectroscopy (AAS), nuclear magnetic resonance spectroscopy (NMR) and electron paramagnetic resonance spectroscopy (EPR) were also performed.

Results and Discussion

Sodium and the PAHs are dissolved in tetrahydrofuran (THF) resulting in dark colored solutions. As already mentioned in literature,[25] naphthalene, anthracene and pyrene solutions show a green, blue and orange-brown color (Figure 1), respectively. After adding 2 eq G2 to the solution, the color of the solution did not change. Dark-colored solids were isolated after drying in vacuum (Scheme 1).

The cation complex to anion ratios were determined by titration of the hydroxide ions formed upon hydrolysis of the salts (Table S1). By adding water to the salt, the carbanion reacts and forms hydroxide ions, excess sodium also reacts to form NaOH. Thus, the total amount of sodium in the salt can be determined via titration. The carbanion content was calculated indirectly. For this purpose, 1,2-dibromo-ethane was added to the salts reacting selectively with the carbanion via a reductive alkylation.[26] Quenching this product with water allows only excess sodium to react, which can then be determined by acid-base-titration. The amount of carbanion can thus be specified by the difference to the total sodium content. For all carbanions, an approximate 1:1 ion ratio was observed, confirming monovalent anions (Table S1). Upon subtraction of the masses of 1 eq PAH and sodium, the residual mass corresponds to 2 eq of diglyme, as expected (Table S1). From liquid phase NMR spectra of the dried solid products (Figure S1), we can prove the absence of THF.

From saturated THF solutions of Na(G2)$_2$pyrenide, highly air- and moisture sensitive, green, block-shaped crystals were isolated which were appropriate for structure determination. Table 1 lists the crystallographic data of the compound collected at 180 K. The atomic coordinates and displacement parameters, as well as selected interatomic distances and angles can be found in the supplementary material (Tables S2–S4). The compound crystallizes in the monoclinic crystal system in the space group $P2_1/c$ (No. 14) with 4 formula units per unit cell.

Interestingly, the pyrene compound has the lowest symmetry of all thus far structurally characterized Na(G2)$_2^+$ stabilized carbanions compared to orthorhombic Na(G2)$_2$peryleneide, crystallizing in $Pna2_1$, and monoclinic Na(G2)$_2$naphthalenide and Na(G2)$_2$anthracenide, crystallizing in $C2/c$.

In analogy to related polycyclic aromatic compounds,[12a] Na(G2)$_2$pyrenide crystallizes as a separated ion pair with the sodium cation coordinated by six oxygen atoms of two diglyme molecules in a distorted octahedral environment. The unit cell contains four ion pairs. One sodium complex and two pyrenide anions, each built by eight crystallographically independent carbon sites, can be found in the asymmetric unit (Figure S2). The shortest nonbonding C–C distance between two anions are d(C–C) = 3.937(6) Å and d(C–C) = 4.083(6) Å and between cation and anion are d(C–C) = 3.425(6) Å and d(C–C) = 3.490(5) Å. These values are in good agreement with comparable compounds and the ion pair can thus be considered fully separated (Figure 2).

The sodium-oxygen distances d(Na–O) = 2.384(2)–2.433(3) Å with a mean distance of d(Na–O) = 2.408(3) Å are in line with comparable G2 coordination complexes found in other radical ion compounds.[12] The distances d(Na–C^{pyr}) to the carbanions are all above 5.173(4) Å, indicating no bonding interactions.[12]

Pyrenide retains its planarity in the reduced state as the C–C–C angles and C–C–C–C torsion angles, within the standard

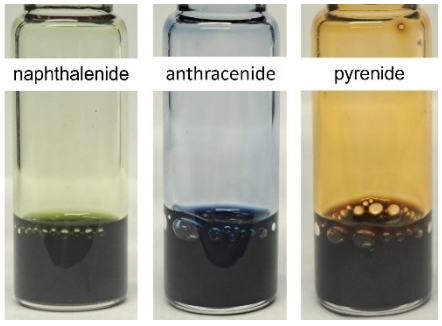

Figure 1. Photographs of the colored sodium carbanion solutions in THF before addition of diglyme.

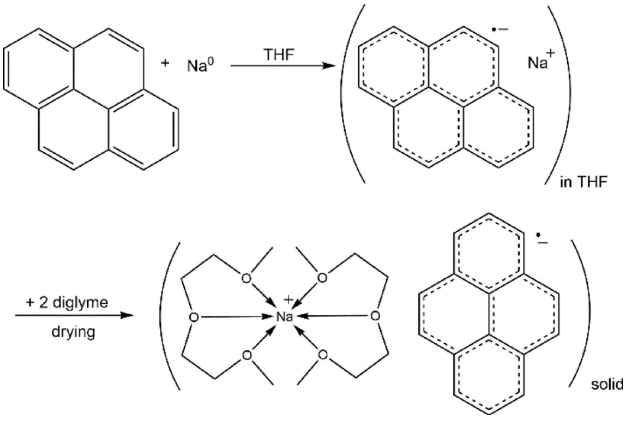

Scheme 1. Reaction of sodium with PAHs in THF exemplary shown for pyrene. After solvating sodium and PAHs, addition of 2 eq diglyme and drying in vacuum resulted in a dark colored solid.

Table 1. Crystallographic data for $Na(G2)_2$pyrenide.[a]

Compound	$Na(C_6H_{14}O_3)_2 \cdot C_{16}H_{10}$
Formula weight M/g·mol^{-1}	493.57
Color/shape	Green block
Crystal size/mm^3	0.05×0.09×0.12
Crystal system, space group	Monoclinic, $P2_1/c$ (No. 14)
Lattice constants from single crystal	
a/Å	8.8459(3)
b/Å	16.4340(7)
c/Å	19.1962(6)
β/°	95.012(3)
Unit cell volume V/Å^3	2780.0(2)
Number of formula units Z	4
Calculated density ρ/g·cm^{-3}	1.179
Diffractometer	STOE STADIVARI
Temperature T/K	180
Wavelength λ/Å	0.71073
Absorption coeff. μ(Mo<C->$K\alpha$)/mm^{-1}	0.094
θ range/°	3.25–25.75
Index range	$-8 \le h \le 10$ $-20 \le k \le 15$ $-22 \le l \le 23$
No. of reflections collected	16416
Independent reflections	5199
R_{int}, R_σ	0.0989, 0.0678
Completeness to $\theta = 25.75°$	97.8 %
Absorption correction	Numerical, X-Area
Structure solution	Intrinsic phasing, ShelXT2018/3
Structure refinement	ShelXL2018/3
Data/restraints/parameters	5199/0/321
GooF, F(000)	0.908, 1060
R_1, wR_2 [$I > 3\sigma(I)$]	0.0558, 0.1143
R_1, wR_2 [all data]	0.1377, 0.1384
Extinction coefficient	0.004(1)
Largest diff. peak & hole/e·Å^{-3}	−0.224, 0.304

[a] Further details of the crystal structure investigation may be obtained from the joint CCDC/FIZ Karlsruhe online deposition service: https://www.ccdc.cam.ac.uk/structures/ by quoting the deposition number CSD-2285829.

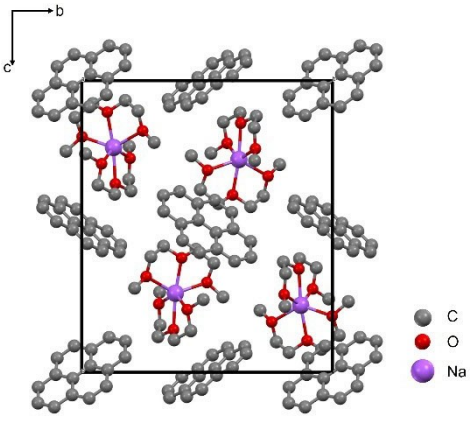

Figure 2. Unit cell contents of $Na(G2)_2$pyrenide viewed along the crystallographic a-axis.

error, do not deviate more from the ideal values of 120° and 180°, respectively, than regular pyrene.[27]

Compared to pyrene,[28] the mean carbon-carbon bond length in $Na(G2)_2$pyrenide do not differ significantly by more than 0.5 %. For the individual C–C bonds, however, some noticeable differences can be observed. These changes are significant enough that even though crystal structure data at reasonably close temperatures is not available, certain trends can be observed. Figure 3 shows a graphical comparison of the bond lengths d(C–C) in pyrene compared to the pyrenide anions found in $Na(G2)_2$pyrenide. In pyrene, the longest bond lengths of d(C–C) > 1.40 Å are observed between carbon atoms connected to three adjacent carbon atoms in the middle of the aromatic ring. Bonds involving only one such "ternary" carbon are slightly shorter at d(C–C)~1.41 Å, while any C–C bond not involving a "ternary" carbon is significantly shorter at d(C–C) ≤ 1.38 Å. Both crystallographically independent pyrenide anions in $Na(G2)_2$pyrenide show the same trend of changes in bond lengths. In general, only the distances closer to the center of the polycyclic system change, while the terminal bonds and the longest C–C bond in the center of the π-system stay the same length. The changes lead to an overall elongation of the pyrenide anion along the longest axis through the center which can be seen well in Figure 3. This observed trend is mostly in line with changes in the bond length in 1D infinite sodium pyrenide chains by Jost et al.[24b] and Näther et al.[24a] Larger differences are observed in the carbon-carbon bonds the sodium cation directly coordinates to. These differences are a lot more pronounced in the lithium compound by Jost et al.[23] and we thus stick to the comparison of the pyrenide anions only with pure pyrene.

Purity of the dried bulk material obtained from the reactions in THF was determined using X-ray powder diffraction (PXRD) and NMR spectroscopy (Figure S1). The PXRD measurement of the pyrenide (Figure 4) showed no discernible impurity phases and further confirms our refined structure model. All reflections could be indexed with a monoclinic unit cell of a = 8.9908(4) Å, b = 16.6367(8) Å, c = 19.1723(7) Å, β = 94.734(2)°, and V = 2857.9(2) Å^3.

In addition to the pyrene compound, we also prepared salts of other PAHs (naphthalene and anthracene) using this synthesis route. This way, it was possible to reproduce the known

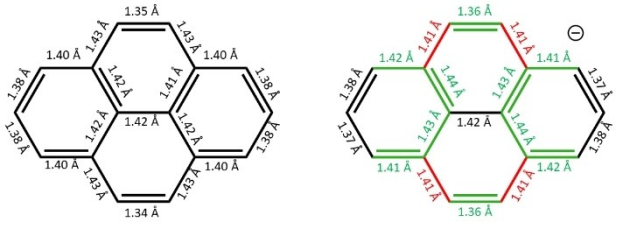

Figure 3. Comparison of the C–C bond lengths in pyrene (left) and one pyrenide anion in $Na(G2)_2$pyrenide (right). Elongating bonds are highlighted in green while shortening bonds are highlighted in red.

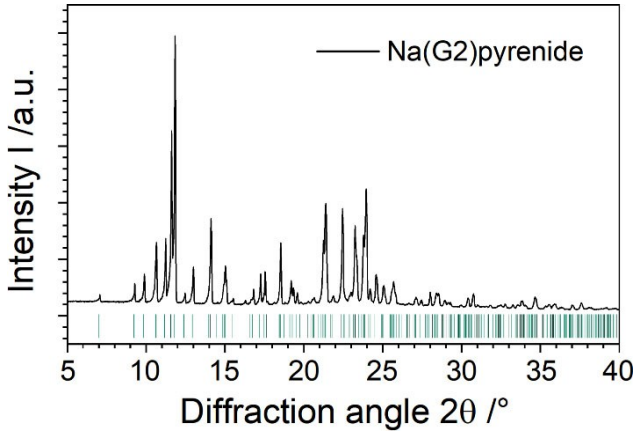

Figure 4. X-ray powder diffraction pattern of Na(G2)$_2$pyrenide (Cu–Kα_1 radiation, 20 °C), confirming phase purity of the bulk sample. Reflection positions based on the single-crystal data (using the room temperature unit cell) are also depicted.

compounds Na(G2)naphthalenide and Na(G2)anthracenide (Figure S3).[12a]

Ambient temperature EPR spectra of all three PAH salts were collected in THF solution (Figure 5) and of the solid samples. All spectra show a singlet signal with unresolved hyperfine coupling. Collected spectra of the solids and the THF solutions at liquid nitrogen temperature can be found in the supplementary information (Figure S4).

Conclusions

Sodium diglyme complexes are stabilizing different aromatic radical carbanions, resulting in reducing agents with varying reduction potentials. In this work, we prepared and structurally characterized Na(G2)pyrenide. In the future, it is planned to apply this synthesis route to other alkali metals and other complexing agents in order to have a wide range of reducing reagents available. These can be used to easily prepare graphite intercalation compounds, which can potentially have application in batteries.

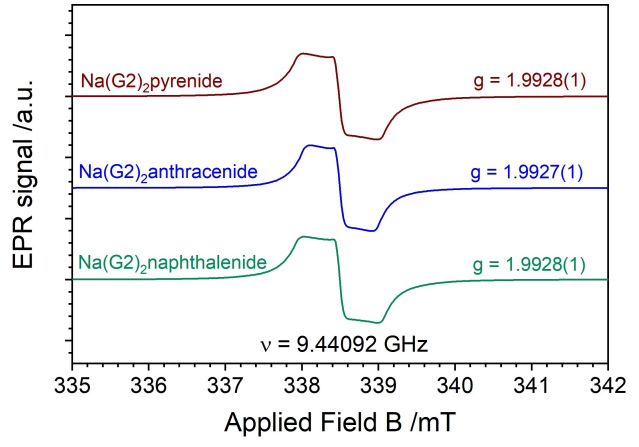

Figure 5. X-band EPR spectra of Na(G2)naphthalenide, Na(G2)anthracenide and Na(G2)pyrenide in THF solution at 20 °C.

Experimental Section

General. All experiments were performed under inert Ar atmosphere by using Schlenk techniques or inside a glovebox. Sodium, naphthalene, anthracene, and pyrene were used as obtained by Sigma-Aldrich without further purification. The anhydrous diglyme was purchased from Sigma-Aldrich and used without any further purification. THF was pre-dried over molecular sieve (4 Å), distilled and stored in a glovebox before usage.

Synthesis of the sodium salts. The PAH (naphthalene, anthracene, or pyrene) and freshly cut sodium were dissolved at a molar ratio of 1:1 in THF overnight. The solutions turned into a greenish, bluish or orange-brownish color for naphthalene, anthracene and pyrene, respectively. In a molar ratio of 1:2 compared to sodium, anhydrous diglyme was added dropwise to the colored solutions. After a reaction time of several hours, the THF was removed by vacuum drying resulting in colored solid phases.

Titration. The overall sodium content was determined by indirect titration of the carbaion and excess elemental sodium. 40–50 mg of the mortared salts were quenched in bidest. water and titrated with 0.05 M HCl. Phenolphthalein was used as indicator. For a more precise determination of the sodium content, the titration was performed twice for each salt. The carbanion concentration was specified by indirect titration by reaction with 1,2-dibromo-ethane. 1 ml of 1,2-dibromo-ethane were added to 20–30 mg of the mortared salts. After a reaction time of 15 minutes, the solution was quenched by 1 ml bidest. water. The titration was performed with 0.05 M HCl and Phenolphthalein as indicator.

Atom absorption spectroscopy. For the AAS analyses, approximatly 20 mg sample was weighed into a clean Teflon flask. After addition of 1.5 mL 30 wt.% HCl, 0.5 mL of 85 wt.% H_3PO_4, 0.5 mL 65 wt.% HNO_3 and 1 mL of 48 wt.% HBF_4 the sample was digested in a MLS 1200 Mega microwave digestion apparatus (MLS GmbH, Mikrowellen-Labor-Systeme, Leutkirch, Germany). The sample was treated for 8 min at 200 W, then for 5 min at 0 W, then for 8 min at 300 W, again for 5 min at 0 W and finally again for 7 min at 600 W and 10 min at 0 W. The closed sample container was cooled to room temperature and the clear solution was diluted by Cs-puffer to 100 mL in a volumetric flask. For better results the samples were again diluted 1:10 with a Cs-puffer before measurement. The measurements were performed at a Varian AA100.

Growth of single-crystals. A small amount of dried Na(G2)$_2$pyrenide was redissolved in THF until a saturated solution was formed and material precipitated. This solution was then subsequently heated to 40 °C in inert gas conditions, the oversaturated solution was separated from the sediment at 40 °C. The solution was sealed in an air-tight container and put in the freezer at −20 °C for a week. Quantitative amounts of crystalline material could be obtained by dripping small amounts of this solution in mineral oil (Paratone N, Hampton Research). Upon quick evaporation of the solvent, block-shaped bright green crystals formed. The crystals quickly decompose in moist air within minutes.

Single-crystal X-ray diffraction. A suitable green, block-shaped single-crystal of $Na(C_6H_{14}O_3)_2 \cdot C_{16}H_{10}$ was mounted on a MiTeGen holder using Paratone N oil (Hampton Research). Diffraction data was collected at 180 K using a STOE STADIVARI equipped with a Dectris Pilatus 200 K CCD detector and a Mo-Kα X-ray source ($\lambda =$

0.71073 Å) The diffraction data was corrected for Lorentz and polarization effects, and the absorption was corrected by a numerical absorption correction (based on the crystal faces) using the X-Area software suite. Within 50° 2θ, the data set had a completeness of 97.9 %.

Crystal structure determination. The crystal structure was solved by intrinsic phasing methods using ShelXT2018/2[29] and refined on F^2 using full-matrix least-squares methods with ShelXL2018/3.[30] Hydrogen positions for aromatic and secondary CH_2 were added with a riding model using fixed geometrical sites for each atom and the diglyme methyl groups were refined as idealised rotating groups. In the final refinement, nine reflections, possibly resulting from ice growth during the experiment, with unreasonable F_{obs}-F_{calc} were omitted. The resulting structure model was checked for missing symmetry and transformed into the standard setting using the PLATON software package.[31]

Powder X-ray diffraction. Powdered samples were sealed in glass capillaries (1.0 mm inner diameter, Hilgenberg) under inert atmosphere. The samples were measured in transmission mode on a STOE Stadi P diffractometer equipped with a Dectris Mythen 1 K detector using monochromatic Cu-Kα_1 radiation ($\lambda = 1.54056$ Å, Ge111 monochromator).

Nuclear magnetic resonance spectroscopy. ^{13}C-NMR spectra were collected on a Bruker Avance 300 spectrometer.

Electron paramagnetic resonance spectroscopy. The X-Band EPR measurements were carried out with a Magnettech GmbH MiniScope MS400 device with a microwave frequency of 9.5 GHz and rectangular resonator. For the measurements, the samples were sealed under Ar gas atmosphere in glass capillaries (inner diameter 0.8 mm). Both, the solid salts and the salt solutions in THF (0.1 M) were analysed by EPR.

Acknowledgements

N. E. thanks the Elite Network of Bavaria (ENB) for a research fellowship and the elite study program "Macromolecular Science" for a fellowship. The authors would like to thank Sonja Lutschinger (University of Bayreuth) for the AAS measurements and Dr. Gábor Balàzs (University of Regensburg) and Helmut Schüller (University of Regensburg, Central Analytical Services) for help with the EPR measurements and instrument time. We would like to thank Dr. Gerald Hörner (University of Bayreuth) for assistance with the single-crystal measurement and Prof. Dr. Rhett Kempe (University of Bayreuth) for instrument time on the single-crystal diffractometer. The authors acknowledge Dr. U. Lacher and K. Hannemann for running NMR measurements. Open Access funding enabled and organized by Projekt DEAL.

Conflict of Interest

The authors declare no conflict of interest.

Data Availability Statement

The data that support the findings of this study are available from the corresponding author upon reasonable request.

Keywords: Aromatic radical Carbanion · Sodium · Digylme · Crystal structure · X-Ray diffraction

[1] A. A. Kebede, T. Kalogiannis, J. Van Mierlo, M. Berecibar, *Renewable Sustainable Energy Rev.* **2022**, *159*, 112213.
[2] a) C. McKerracher, A. O'Donovan, N. Soulopoulos, G. Andrew, J. Lyu, M. Siyi, D. Doherty, R. C. Fisher, Corey, M. A. Yang, Kwasi, Y. Sekine, A. Leach, E. Stoikou, J. Shi, P. Xu, L. M. Yague, A. Haring, P. Geurts, C. Adraenssens, A. T. Abraham, K. Kareer, https://about.bnef.com/electric-vehicle-outlook/, **2023**; b) H. Deng, K. E. Aifantis, *Rechargeable Ion Batteries* **2023**, 83–103.
[3] a) J. Muldoon, C. B. Bucur, T. Gregory, *Chem. Rev.* **2014**, *114*, 11683–11720; b) Y. Wang, R. Chen, T. Chen, H. Lv, G. Zhu, L. Ma, C. Wang, Z. Jin, J. Liu, *Energy Storage Mater.* **2016**, *4*, 103–129; c) J. W. Choi, D. Aurbach, *Nat. Rev. Mater.* **2016**, *1*, 16013.
[4] C. Vaalma, D. Buchholz, M. Weil, S. Passerini, *Nat. Rev. Mater.* **2018**, *3*, 18013.
[5] K. Chayambuka, G. Mulder, D. L. Danilov, P. H. L. Notten, *Adv. Energy Mater.* **2020**, *10*, 2001310.
[6] a) P. U. Nzereogu, A. D. Omah, F. I. Ezema, E. I. Iwuoha, A. C. Nwanya, *Appl. Surf. Sci.* **2022**, *9*, 100233; b) H. Zhang, Y. Yang, D. Ren, L. Wang, X. He, *Energy Storage Mater.* **2021**, *36*, 147–170; c) S. Komaba, T. Itabashi, M. Watanabe, H. Groult, N. Kumagai, *J. Electrochem. Soc.* **2007**, *154*, A322.
[7] a) K. Nobuhara, H. Nakayama, M. Nose, S. Nakanishi, H. Iba, *J. Power Sources* **2013**, *243*, 585–587; b) O. Lenchuk, P. Adelhelm, D. Mollenhauer, *Phys. Chem. Chem. Phys.* **2019**, *21*, 19378–19390.
[8] a) H. Kim, J. Hong, Y.-U. Park, J. Kim, I. Hwang, K. Kang, *Adv. Funct. Mater.* **2015**, *25*, 534–541; b) B. Jache, J. O. Binder, T. Abe, P. Adelhelm, *Phys. Chem. Chem. Phys.* **2016**, *18*, 14299–14316; c) Y. Li, Y. Lu, P. Adelhelm, M.-M. Titirici, Y.-S. Hu, *Chem. Soc. Rev.* **2019**, *48*, 4655–4687.
[9] B. Jache, P. Adelhelm, *Angew. Chem. Int. Ed.* **2014**, *53*, 10169–10173.
[10] S. Tsuzuki, T. Mandai, S. Suzuki, W. Shinoda, T. Nakamura, T. Morishita, K. Ueno, S. Seki, Y. Umebayashi, K. Dokko, M. Watanabe, *Phys. Chem. Chem. Phys.* **2017**, *19*, 18262–18272.
[11] a) S. N. Spisak, A. V. Zabula, M. V. Ferguson, A. S. Filatov, M. A. Petrukhina, *Organometallics* **2013**, *32*, 538–543; b) R. Michel, R. Herbst-Irmer, D. Stalke, *Organometallics* **2011**, *30*, 4379–4386; c) S. Neander, J. Körnich, F. Olbrich, *J. Organomet. Chem.* **2002**, *656*, 89–96.
[12] a) H. Bock, C. Arad, C. Näther, Z. Havlas, *J. Chem. Soc. Chem. Commun.* **1995**, 2393–2394; b) H. Bock, C. Naether, Z. Havlas, *J. Am. Chem. Soc.* **1995**, *117*, 3869–3870.
[13] A. T. Lawal, *Cogent Environ. Sci.* **2017**, *3*, 1339841.
[14] a) M. Szwarc, M. Levy, R. Milkovich, *J. Am. Chem. Soc.* **1956**, *78*, 2656–2657; b) A. V. Tobolsky, D. B. Hartley, *J. Am. Chem. Soc.* **1962**, *84*, 1391–1393.
[15] a) M. Etienne, R. Choukroun, D. Gervais, *J. Chem. Soc. Dalton Trans.* **1984**, 915–917; b) M. F. Lappert, C. L. Raston, G. L. Rowbottom, B. W. Skelton, A. H. White, *J. Chem. Soc. Dalton Trans.* **1984**, 883–891; c) J. M. Maher, R. P. Beatty, N. J. Cooper, *Organometallics* **1985**, *4*, 1354–1361.
[16] G. P. Moss, P. A. S. Smith, D. Tavernier, *Pure Appl. Chem.* **1995**, *67*, 1307–1375.
[17] D. Eisenberg, R. Shenhar, *Wiley Interdiscip. Rev.: Comput. Mol. Sci.* **2012**, *2*, 525–547.
[18] M. Berthelot, *Ann. Chem. Pharm.* **1867**, *143*, 97–100.
[19] a) L. D. Betowski, M. Enlow, L. Riddick, D. H. Aue, *J. Phys. Chem. A* **2006**, *110*, 12927–12946; b) Y. Okamoto, *J. Phys. Chem. C* **2014**, *118*, 16–19.
[20] a) T. A. Scott, B. A. Ooro, D. J. Collins, M. Shatruk, A. Yakovenko, K. R. Dunbar, H.-C. Zhou, *Chem. Commun.* **2009**, 65–67; b) H.

Bock, K. Gharagozloo-Hubmann, M. Sievert, T. Prisner, Z. Havlas, *Nature* **2000**, *404*, 267–269.
[21] M. Castillo, A. J. Metta-Magaña, S. Fortier, *New J. Chem.* **2016**, *40*, 1923–1926.
[22] N. Eichstaedt, K. P. v. d. Zwan, L. Mayr, R. Siegel, J. Senker, J. Breu, *Z. Naturforsch. B* **2021**.
[23] W. Jost, M. Adam, V. Enkelmann, K. Müllen, *CSD Communication* **1997**.
[24] a) C. Näther, H. Bock, R. F. C. Claridge, *Helv. Chim. Acta* **1996**, *79*, 84–91; b) W. Jost, M. Adam, V. Enkelmann, K. Müllen, *Angew. Chem. Int. Ed.* **1992**, *31*, 878–879.
[25] P. Balk, G. J. Hoijtink, J. W. H. Schreurs, *Recl. Trav. Chim. Pays-Bas* **1957**, *76*, 813–823.
[26] K. Müllen, *Angew. Chem.* **1987**, *99*, 192–205.
[27] A. Camerman, J. Trotter, *Acta Crystallogr.* **1965**, *18*, 636–643.
[28] a) X. Pang, H. Wang, W. Wang, W. J. Jin, *Crystal Growth* **2015**, *15*, 4938–4945; b) A. Matsumoto, M. Suzuki, H. Hayashi, D. Kuzuhara, J. Yuasa, T. Kawai, N. Aratani, H. Yamada, *Chem. Eur. J.* **2016**, *22*, 14462–14466.
[29] G. Sheldrick, *Acta Crystallogr. Sect. A* **2015**, *71*, 3–8.
[30] G. Sheldrick, *University of Göttingen, Göttingen, Germany* **1997**.
[31] A. L. Spek, *J. Appl. Crystallogr.* **2003**, *36*, 7–13.

Manuscript received: August 1, 2023
Revised manuscript received: October 17, 2023
Accepted manuscript online: November 7, 2023

